Gas accumulation in particle-rich suspensions and implications for bubble populations in crystal-rich magma

Isolde B. Belien *, Katharine V. Cashman, Alan W. Rempel

Department of Geological Sciences, 1272 University of Oregon, Eugene, OR 97403, USA

ARTICLE INFO

ABSTRACT

Gas mobility plays an important role in driving volcanic eruptions and controlling eruption style. The explosivity of an eruption depends, among other factors, on how easily gas can escape from the magma. Many magmatic systems have high concentrations of suspended crystals that inhibit gas migration through the melt. We use suspensions of plastic beads in corn syrup to investigate interactions between rising bubbles and particles. We observe different interaction styles as the ratio ψ of bubble to particle size is varied. Large bubbles ($\psi>1$) deform and sometimes break up as they move around particles. Small bubbles ($\psi<1$) are frequently trapped within the suspension, increasing the concentration of gas held within the system. We compare our experiments to bubble populations in tephra from Stromboli volcano, Italy. We show that these samples typically have bubbles and crystals of similar sizes and suggest that crystals might play a role in controlling bubble size in this natural system as well as in our experiments. Because small bubbles ($\psi<1$) get trapped within the suspension, and can be formed by breakup of larger bubbles, we expect that an increase in gas flux will result in an increase in the population of small bubbles. Changes in bubble number density and vesicularity in tephra erupted during periods of different eruptive intensity may thus provide a way of tracking changes in gas flux through the magma prior to eruption.

© 2010 Elsevier B.V. All rights reserved.

1. Introduction

Mafic eruptions are commonly interpreted using results of two-phase flow experiments (e.g. Vergniolle and Mangan, 2000). However, many volcanic systems include three phases (solid, liquid, gas), where the crystals present in suspension may influence the rise of gas bubbles. If the crystal concentration is low, the crystal-liquid mixture can be treated as a fluid with higher effective density and viscosity than the liquid phase alone, slowing bubble rise. If the crystal concentration is high, however, crystals might not be able to move freely, and the effect of solids on gas bubbles could be more complicated. In this study, we use analogue experiments to investigate the influence of particles on bubble populations in low Reynolds number (viscous) systems with high particle concentrations (~50% by volume). We focus on the dynamics of small bubbles in viscous suspensions, and examine what this can tell us about gas flux. We apply our results to Stromboli volcano, Italy, where the crystallinity is similar to the particle concentrations in our experiments, and gas rises through a mostly stagnant magma.

Experiments similar to ours have been done in high Reynolds number systems in chemical engineering. In these systems, the local percentage of gas in the system (termed gas holdup) generally decreases with increasing solids concentration because of an increase in particle-aided bubble coalescence. However, these studies demonstrate that the effect of particles on gas holdup is complicated and depends on both particle size and concentration (see Mena et al., 2005, for an overview). Here, we focus on the low Reynolds number equivalent, where inertia is negligible.

We compare the results of our experiments to bubble and crystal populations observed in tephra from Stromboli volcano. At Stromboli, gas migration through a shallow crystal-rich magma produces ~13 megatons of gas per day, of which only 10% is accompanied by eruption of volcanic rocks (Harris and Ripepe, 2007). These Strombolian eruptions occur every 10–15 min and eject tephra and ash to heights of a few hundred meters. Non-eruptive active degassing episodes (puffing) account for another 45% of the gas (Harris and Ripepe, 2007). These events are frequent (~ every 2 s) and produce pressure pulses of ~10^3 Pa at the vent (Ripepe et al., 2007). The remaining ~45% of degassing is completely passive. This shows that the overall gas flux at Stromboli far outstrips the magma flux.

At Stromboli, two magmas are inferred to exist at depth. They have similar, high potassium–basaltic compositions but differ in crystal content. Tephra erupted during normal Strombolian activity derives

* Corresponding author. Tel.: +1 541 346 5989; fax: +1 541 346 4692.
  E-mail address: ibelien@uoregon.edu (I.B. Belien).

from magma with a crystallinity of approximately 50%. This (shallow) magma resides above a more volatile-rich and crystal-poor magma that is erupted as pumice during infrequent paroxysms (e.g. Bertagnini et al., 2003; Landi et al., 2004).

To investigate the mechanisms of small bubble migration through a crystal-rich, essentially stagnant magma such as at Stromboli, we perform analogue experiments using solid particles (plastic beads), gas (air bubbles) and a viscous fluid (corn syrup). We use different experimental setups to study 1) the influence of solid particles on the rise of a single bubble and 2) the influence of solid particles on bubble populations. In what follows, we first discuss our analogue experiments. We then use our experimental results to interpret bubble populations in crystal-rich tephra from Stromboli. We discuss the applicability of our experiments to Stromboli through a comparison of dimensionless parameters in both systems. We then combine our experimental results with data from the literature to speculate on the effect of gas flux on bubble populations at Stromboli.

2. Experiments and observations

We examine the rise of small bubbles through a viscous suspension using analogue experiments. The physical properties of the materials used in these experiments are listed in Table 1. Below, we first describe the setup and then the observations for three different sets of experiments. The first two examine how a single rising bubble interacts with particles. The third experiment examines the interactions of a stream of bubbles with particles.

2.1. Individual bubbles

The setup for the first set of experiments consists of a Plexiglas tank with a syringe and needle connected to the bottom (Fig. 1a). The tank is 15 cm wide, 25 cm tall and narrow (1.5 cm) in the third dimension (a Hele–Shaw cell) to ensure visibility through the particle layer. A randomly packed layer of plastic cubes with 7 mm sides was suspended on the interface between two types of corn syrup with different densities and viscosities (Table 1). The particle concentration in the suspension was approximately 50% by volume. The thickness of the particle layer was varied between 1 and 10 cm. Air injected into the system from below produced bubble sizes of 0.1 to 1 ml (bubble: particle width ratio ψ between 0.8 and 1.8). Measured wetting angles indicate that, in common with magmatic systems, the liquid phase preferentially wets the solid particles.

Increasing the bubble size relative to the particle size causes the interaction style to change (Fig. 2). When the bubble is much smaller
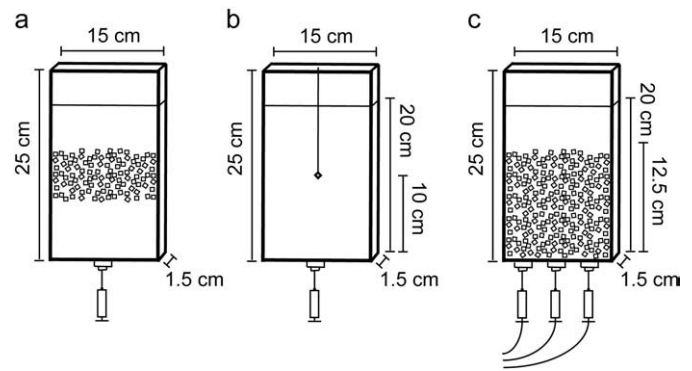

Fig. 1. Schematic of setups used to study a) styles of interaction between a single bubble and particles in suspension, b) occurrence frequency of different interaction styles between a single bubble and a single particle, and c) the effect of a particle suspension on bubble size distributions.

than the pores in the suspension, it rises through the pores without displacing the particles and undergoes only minimal deformation (Fig. 2a). The speed of bubble rise varies along its contorted pathway around the particles. Very small bubbles sometimes stall completely beneath a particle, so that they are effectively trapped within the suspension. When the bubble is large and the particle layer is thin, the bubble can displace the particles in such a way that the bubble deformation remains small relative to the deformation of the suspension layer (Fig. 2d). When the particle layer is thick and the bubble is too large to move between particles without deforming, it can either elongate to move through the pores (Fig. 2b), or flatten underneath an individual particle. After a bubble flattens, it may either move around the particle or split into two or more parts (Fig. 2c) to create new bubbles that are sufficiently small to move through available pores in the network. The specific response depends on particle orientation (flat side down or edge down), position relative to the bubble (in the middle; towards the edge), and the bubble:particle size ratio ψ.

2.2. Splitting probabilities

We determined probabilities of different interaction styles between a single bubble and a single particle in a setup in which a particle was suspended from a metal rod into the low viscosity syrup (Fig. 1b). We injected a single bubble into the syrup approximately

Table 1
Properties of materials used in this study compared to natural systems. ρ: density, η: viscosity, V_b: bubble volume, d: bubble equivalent diameter, σ: surface tension, w: particle width, α: gas–solid wetting angle. Liquid properties for this study are measured at room temperature. [a] Value for the light syrup; the dense syrup was too sticky for the apparatus and its σ could not be measured. [b] Stromboli ρ: from Métrich et al. (2001) and Bertagnini et al. (2003) from glass in melt inclusions in pumice, η: calculated from compositional data for glassy matrices in crystal-rich scoria in Landi et al. (2004) using the method of Shaw (1972) with 0.1 weight% H_2O and T = 1115 °C (Landi et al., 2008) (not corrected for the influence of crystals), σ: based on Khitarov et al. (1979), d and w: dominant bubble and crystal sizes from Fig. 5a. Note that ρ and η are measured or calculated for glass and not corrected for the influence of crystals, and thus represent the density and viscosity of the melt phase alone and not the bulk magma. [c] Approximate volatile-free values at 1 bar, based on Spera (2000). [d] Basalt values from Khitarov et al. (1979). [e] Compositions ranging from dacite to synthetic haplogranite, from Bagdassarov et al. (2000) and Mangan and Sisson (2005). Wetting angles are measured on photos for experiments. SEM images for Stromboli show thin glass (melt) films between bubbles and crystals, indicating that the melt preferentially wets the crystals (0° wetting angle).

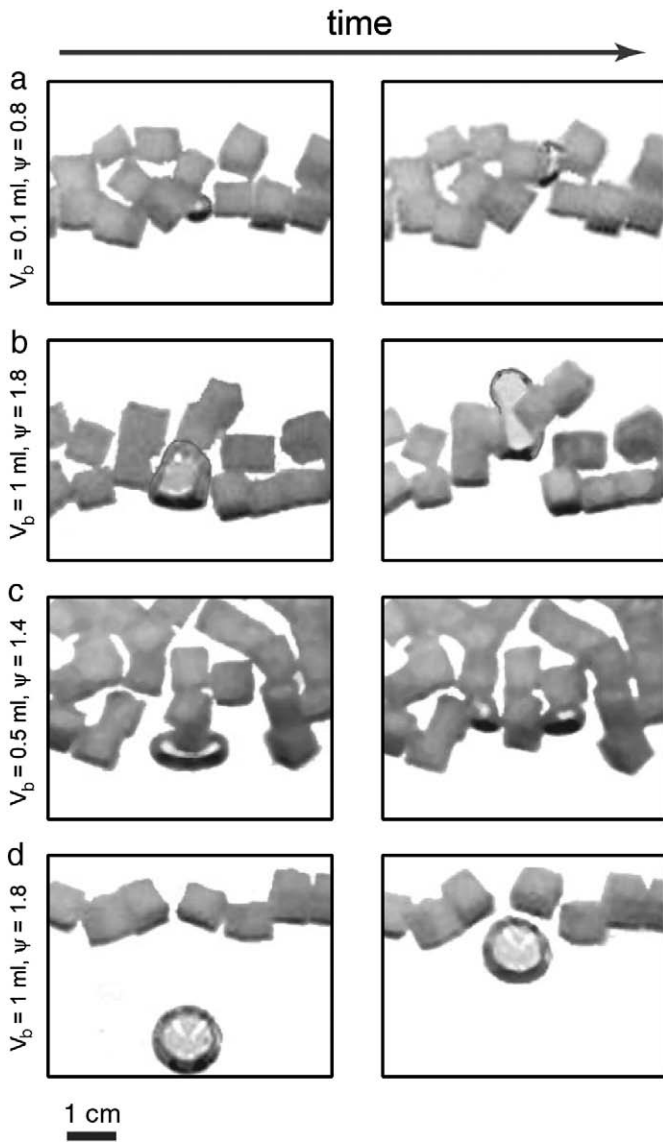|		This study	Mafic magma Stromboli[b]	Mafic magma	Silicic magma	Seawater
Liquid	ρ (kg/m³)	Light syrup: 1320 Dense syrup: 1421	2690	2500–2700[c]	2350–2450[c]	1000
	η (Pa s)	Light syrup: 4.12 Dense syrup: 20	330	10^1–$10^{3\,c}$	10^5–$10^{10\,c}$	0.0018
Gas	V_b (ml)	0.1–1				
	d (mm)	5.8–12.4	0.1–0.3			
Liquid + gas	σ (N/m)	0.071[a]	0.1–0.4	0.09–0.4[d]	0.042–0.3[e]	0.072
Solid	w (mm)	7	0.1–0.3			
Liquid + gas + solid	α (°)	10–30	0			

Fig. 2. Styles of interaction between a bubble and particles suspended in a viscous fluid. Interaction style changes from a to b/c with increasing bubble volume. d occurs when bubbles are large and particles can move freely. See text for details.

10 cm below the particle, and tracked, through repeat experiments, how often the bubble was stuck, split around the particle, or moved around the particle without splitting. A bubble was considered stuck when it remained trapped beneath the particle for more than 2 min (during which time our smallest (0.1 ml) bubbles could rise almost 70 cm if unhindered). A bubble was considered split when it broke into smaller bubbles as a result of interacting with the particle. If these smaller bubbles were similar in size to each other, they usually ascended on opposite sides of the particle. If one part was much larger than the other part, the smaller part remained close to the particle for long periods of time, moving slowly up its side (either the same or the opposite side as the large part of the bubble). Small bubbles from different splitting events accumulated close to the particle. A bubble was considered complete when it moved around the particle without splitting.

We varied bubble size between 0.1 and 1 ml ($0.8 \leq \psi \leq 1.8$) and performed these experiments with the particle orientation both flat side facing down and edge facing down, to examine how the frequency of occurrence of each interaction style changes with bubble volume and particle orientation. Each experiment was repeated 50 times to obtain statistically meaningful results, which are shown in Fig. 3.

Our experiments show that the probability of the smallest bubbles getting stuck underneath the particle is approximately 60% when the particle is oriented flat side down. In experiments with a suspension this probability would be higher, since bubbles could also become trapped beneath clusters of particles (assuming these could not be pushed aside easily by the bubble). Bubbles did not stagnate beneath particles oriented with the edge pointed down. The probability of stagnation decreases dramatically with bubble size, while the probability that a bubble will split around the particle increases with bubble size. Bubbles are more likely to split when the particle is oriented with an edge facing downward. Both the generation of small bubbles from large ones by splitting and the high probability of small bubbles remaining trapped beneath particles indicate that there should be a relative enrichment of small bubbles in high-crystallinity systems.

2.3. Bubble populations

To study the effect of solid particles on bubble populations in a system that is fluxed with gas, we used a similar setup to that used in the first set of experiments, except that it included three injection ports at the base of the tank (Fig. 1c). We injected bubbles from three nozzles simultaneously every 10 s. The experiments were videotaped and individual movie frames analyzed with the image analysis software ImageJ (Abramoff et al., 2004). The size distribution of bubbles present in the system was determined from movie frames extracted at set time intervals after the start of injection of the bubble
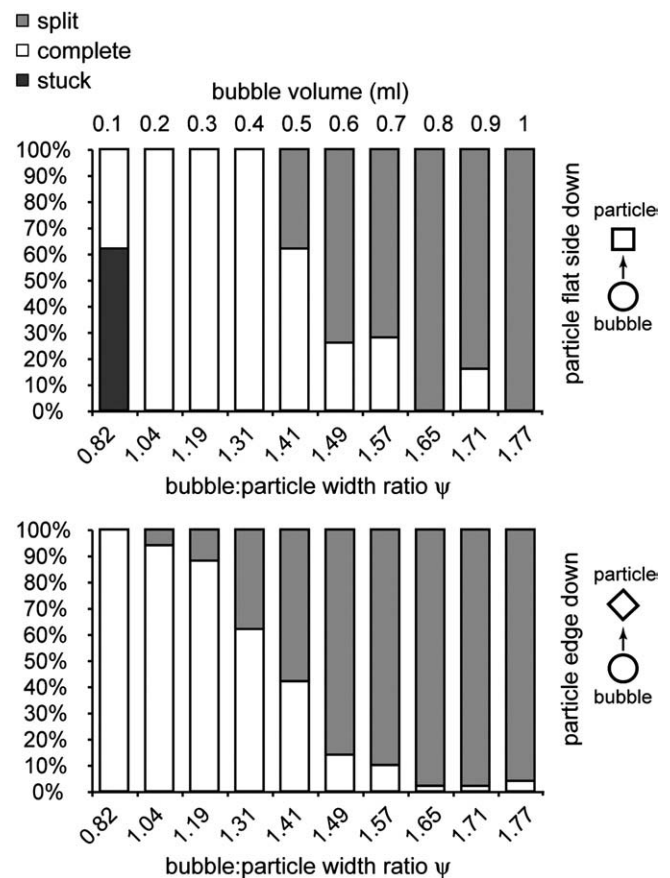

Fig. 3. Occurrence frequencies of interaction styles between a single particle and a single bubble injected directly underneath for different particle orientations. Top: flat side down, bottom: edge down.

stream. Only the low density, low viscosity syrup was used in these experiments to avoid mixing of the syrups by moving bubbles. The particles are more dense than the syrup and formed a randomly packed, 12.5 cm thick layer at the bottom of the tank. The particle concentration was approximately 50% by volume, which is comparable to the solid concentrations in high-crystallinity magmas.

At the start of each experiment, some bubbles trapped during creation of the suspension were present in the system. These were flushed out by repeated bubble injections, as indicated by the measured bubble size distribution, which narrowed with time to a distribution around the input bubble size (see Supplementary Fig. 1 for an example).

Fig. 4 shows histograms from movie frames taken near the end of each experiment, when the spread is assumed to have reached its steady-state width. The gray area represents the spread expected in the absence of splitting or coalescence and is instead due to bubbles appearing smaller when they are partly hidden behind particles and larger when they are flattened between a particle and the front wall of the tank. This spread may be determined from the 0.1 ml experiment, where no splitting or coalescence was observed. Small bubbles become increasingly abundant as the input bubble size increases, indicating frequent bubble breakup. In contrast, bubble coalescence appears almost negligible. When coalescence was observed, it usually happened as bubbles were exiting the particle layer.
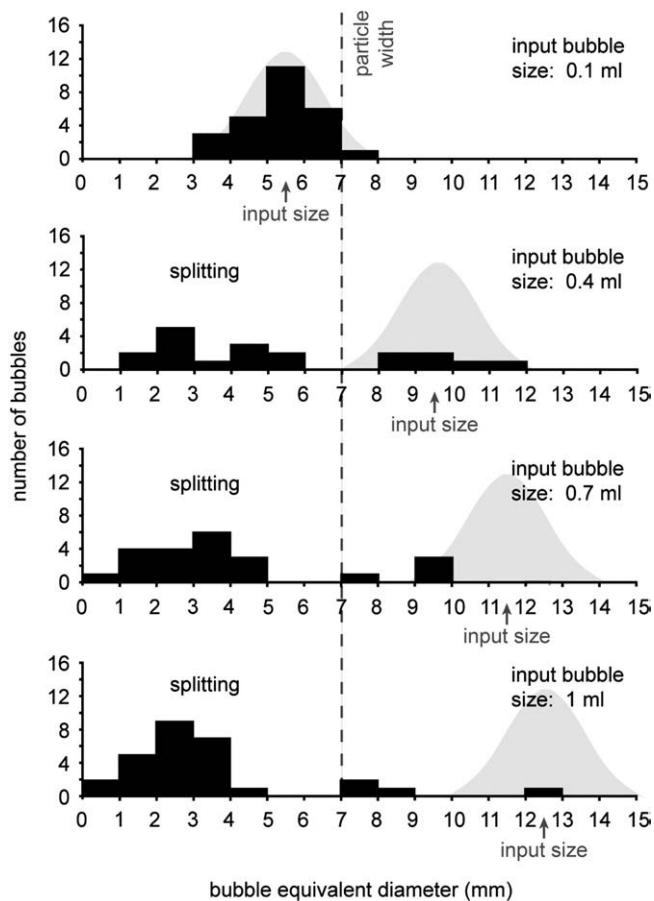
Fig. 4. Steady-state size distributions of bubbles inside a particle suspension resulting from through-flux of bubbles of a single size, for bubble input sizes of 0.1, 0.4, 0.7 and 1 ml. The gray area represents the apparent distribution expected if the bubbles in the suspension are all the input size, based on the 0.1 ml experiment, in which no splitting or coalescence was observed. Bubbles to the left of the distribution are smaller than the input size. Bubbles to the right of the distribution are larger than the input size (not observed inside the suspension). Small bubbles form by splitting of larger bubbles around the particles. Splitting is more likely for larger bubbles, and the number of small bubbles in the suspension increases with bubble input size.

2.4. Summary of experimental observations

Our experiments show that bubbles interact with suspended particles in different ways (Section 2.1 and Fig. 2) depending on the size of the bubble relative to the pore size (which depends on particle size, shape and concentration). Small bubbles move through the pores without deforming, and can stagnate beneath particles. Bubbles that are wider than the pores may deform to move between particles. If the particles do not block each other's movement, they can be displaced to a limited extent by the rising bubble.

Particles can cause large bubbles ($\psi > 1$) to split into smaller ones. The frequency of breakup is highest for large bubble:particle width ratios (Section 2.2 and Fig. 3) and decreases rapidly with decreasing bubble size. Breakup occurs for all particle orientations, but is most pronounced when the particle is oriented edge down. In our single particle experiments, only bubbles that were smaller than the width of the particle could stagnate beneath it, and stagnation occurred only when the particle was oriented with its flat side down.

When multiple bubbles of the same starting size rise through a particle suspension (Section 2.3 and Fig. 4), the concentration of small bubbles generated by bubble breakup increases with increasing bubble input size. This observation lends support to our inference that breakup occurs more frequently for larger bubble:particle size ratios.

From these results we infer that in a particle-rich suspension, the combined effects of small bubble generation by breakup of large bubbles and stagnation of small bubbles beneath particles can produce enrichment of small bubbles relative to larger ones. Even in the absence of particles, the lower rise rates of small bubbles relative to larger ones can drive the relative enrichment of small bubbles in any given volume (e.g. Cashman et al., 1994). Bubbles of all sizes rise more slowly through a suspension than they would in the absence of particles. (See Supplementary Fig. 2 for rise rates with and without particles in our experimental setup.) However, only the smallest bubbles stagnate completely inside the suspension. We suggest that vesicle populations in mafic systems where gas flux greatly exceeds magma flux, such as Stromboli volcano, will record an integrated history of both primary vesiculation processes and modifications produced by gas movement relative to the magma.

3. Bubble populations in tephra from Stromboli

To assess the applicability of our experiments to mafic volcanoes, we compare our experimental results to bubble populations within tephra from Stromboli volcano, where gas moves through magma with a crystallinity of ~50% (e.g. Métrich et al., 2001; Armienti et al., 2007), close to the particle concentration in our analogue system. We collected 3 samples from a single explosion during a series of ash-rich eruptions on 19 July 2007. These eruptions represented renewal of normal Strombolian activity after a pause in activity that followed a large eruption on 15 March 2007. At this time, explosions from the northern crater generated 4–5 ash plumes per hour, with an average height of 100–150 m above the vent (http://www.ct.ingv.it/stromboli2007/main. htm). Our samples have vesicle-free crystallinities of ~30–40% by area and crystal-free vesicularities of ~15–60%. Crystals range in size from approximately 50 μm to 2 mm. Bubbles range in size from approximately 10 μm to 3 mm, and have complex shapes.

Crystal and bubble size distributions of one sample are shown in Fig. 5, as determined from binary images created from both digitized thin section and scanning electron microscope (SEM) images. Fig. 5a shows the number of bubbles and crystals of different sizes per unit area in the thin section scan. The size of the bubbles is expressed as equivalent diameter d, which is calculated from the area A_b of each bubble as $d = 2\sqrt{(A_b/\pi)}$. The size of the crystals is expressed as equivalent width w, which is calculated from the area A_c of each crystal as $w = \sqrt{(A_c)}$. Since the resolution of the thin section scans is
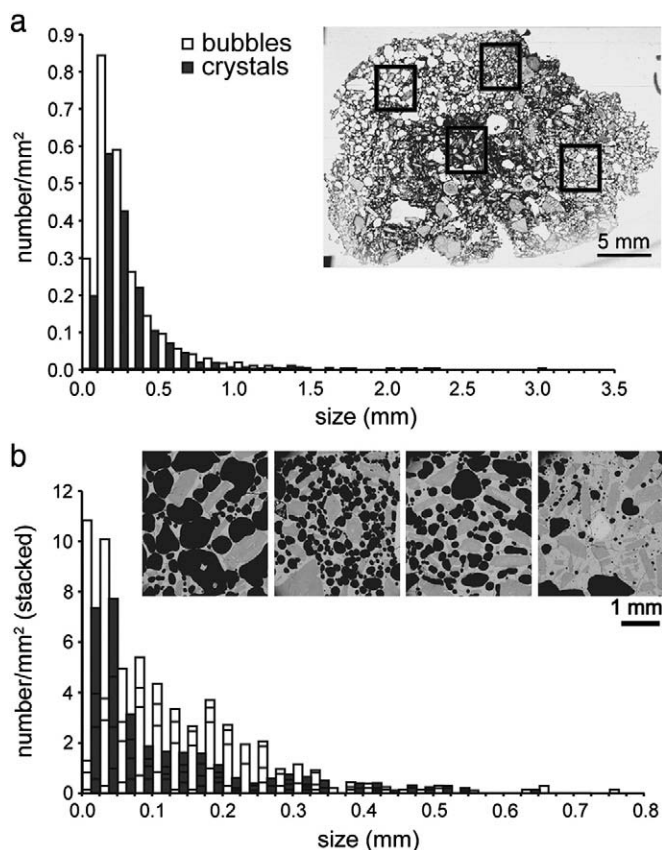
Fig. 5. Bubble and crystal size distributions (normalized to total area of melt + crystals + bubbles) in a thin section scan (a) and on 39× magnification SEM images from the same thin section (b). The analyses for the SEM images are stacked in the histogram (b), with the analysis for the leftmost image on the bottom and the analysis for the righthand image on the top. The location of the SEM images in the thin section scan is shown by the black boxes. Bubble size is calculated from the area A_b as $d = 2\sqrt{(A_b/\pi)}$. Crystal size is calculated from the area A_c as $w = \sqrt{(A_c)}$. The y-axis indicates the number of bubbles or crystals of a certain size present per area unit of the analyzed image. The SEM images represent areas with different textures present within the thin section scan (locations shown by black boxes). Note that bubbles appear white on the thin section image and black on the SEM images.

not high enough to analyze the smallest bubbles and crystals, we used SEM images to characterize these. Fig. 5b shows analyses (stacked in the histogram) for SEM images of different regions of the thin section in Fig. 5a. Microlites are excluded from the crystal population in all these analyses, as they are interpreted to have crystallized rapidly on or immediately prior to eruption, and thus would not have been present in the magma to influence bubble migration.

The bubble and crystal size distributions in each image are similar, indicating that coexisting bubble and crystal populations are similar on both scales and across the range of different textures represented by the SEM images. Although the absolute bubble and crystal size ranges overlap, the bubble distribution in most cases has a broader peak, which is shifted to larger sizes relative to the peak in the crystal distribution and could indicate modest bubble expansion on eruption. This is consistent with conclusions drawn from a comparison of dimensionless parameters in our experiments and in magma (Section 4), as well as with observations of bubble shapes.

Fig. 6 shows SEM images of representative areas in our samples, illustrating the wide variety of bubble shapes and relationships of bubbles to crystals observed in these samples. Fig. 6a shows recently coalesced bubbles, which are readily identified by cusps that remain unretracted (white arrows). Since the bubble walls have not relaxed to a rounded shape, we assume that these bubbles coalesced upon eruption due to expansion, and the bubbles did not have time to relax before the sample quenched (that is, these bubbles were present as

separate, un-coalesced, bubbles in the magma before eruption). Fig. 6b shows a bubble (marked by a gray x) that is deformed but does not have angular cusps and is not clearly bounded by crystals. Assuming its shape was not significantly modified on eruption, this bubble could have formed by coalescence of smaller bubbles in the volcanic conduit, leaving enough time for the cusps to retract but not enough time for the bubbles to relax completely back to spherical. Fig. 6c and d show bubbles (marked by a white x) that are deformed and fill the space between crystals (Fig. 6c) or are bent around crystals (Fig. 6d). In light of our experimental results, we interpret these as having deformed because of the crystals. In fact, they are close to the size of the phenocrysts ($\psi \sim 1$). The rest of the bubble population in these samples consists of small (i.e. $\psi \ll 1$), usually spherical bubbles. Our experiments indicate that small spherical bubbles, which are often interpreted to have formed during a late stage of nucleation, could also have been formed by splitting of larger bubbles. These small bubbles are then enriched in the system relative to larger ones because of their slower rise velocity and tendency to stagnate beneath the particles. Supplementary Fig. 3 shows additional examples of deformed bubbles in SEM images.

These results show that bubble populations in our experimental system and in Stromboli tephra compare qualitatively. To make a better comparison of the two systems, we use dimensional analysis.

4. Comparison of experimental and volcanic conditions

Table 1 compares fluid properties in our experiments and in natural systems. Both viscosity and surface tension are higher in magmatic systems than in our experiments. Higher viscosity implies that both bubble rise and the rate of liquid drainage out of thin films between bubbles or a bubble and a crystal will be slower, increasing time scales for gas movement, bubble splitting and coalescence. Higher surface tension between the bubble and the liquid means that bubbles will be less deformable, and we consequently expect less bubble deformation and breakup in magma than in our analogue experiments. As noted above, wetting angles between bubbles and particles in our experimental system are small; a thin layer of glass is also present between bubbles and crystals in our thin section images, indicating that the liquid preferentially wets the particles in both systems.

Table 2 compares our experimental system and Stromboli magma in terms of bubble and particle sizes and the ratios of forces acting on the bubbles. The size ratio ψ of bubble to particle widths in our experiments falls within the range found in the 2007 Stromboli samples. Note that bubble and particle widths are calculated from three-dimensional data in our experiments whereas they are calculated from two-dimensional bubble and crystal areas observed in Stromboli thin sections, and that we use only the most abundant bubble and crystal sizes occurring in the tephra in our comparison. Bubbles for which $\psi < 0.3$ do exist at Stromboli but are always spherical. Since we are making a comparison with experiments in which all bubbles except the smallest ones deform, we can justify neglecting these smallest size classes. Large bubbles in Stromboli samples deform primarily around larger crystals. The abundance of large bubbles and crystals decreases rapidly with size (Fig. 5a) and for the sake of comparison we ignore this larger tail to the distribution as well.

The other dimensionless parameters shown in Table 2 measure the relative importance of buoyancy, inertia forces, viscous forces and surface tension forces acting on the bubbles. Velocities used to calculate Re and We are measured for our experiments (particle free) and calculated using Stokes flow ($u = r^2 \rho g / 3\eta$) for Stromboli magma. The values of the Reynolds number Re, which describes the ratio of inertial forces to viscous forces, and the Weber number We, which is the ratio of inertia to surface tension, show that inertial forces are unimportant in both our experiments and in magmatic systems.
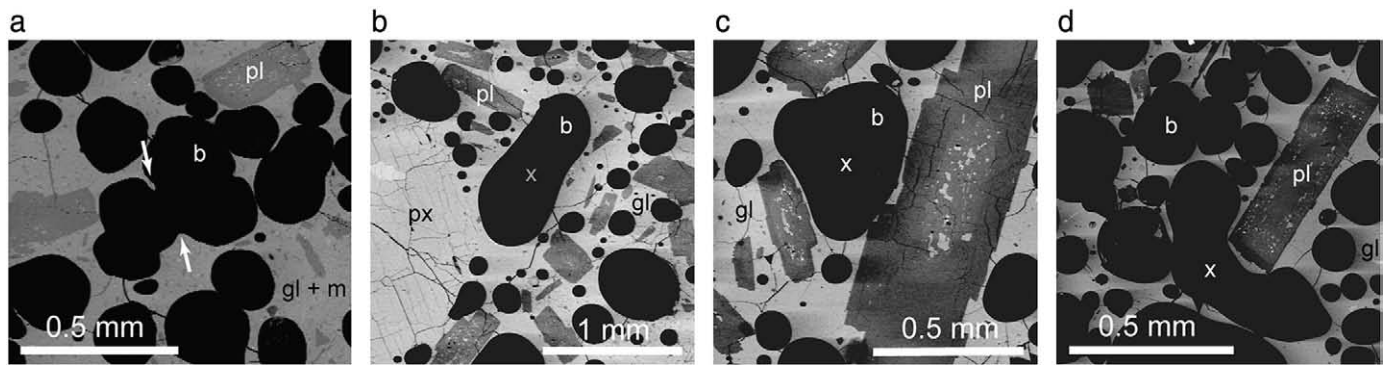
Fig. 6. SEM (scanning electron microscope) images of tephra from Stromboli volcano. b = bubble; pl = plagioclase crystal; px = pyroxene crystal; m = microlites; gl = glass. See text for discussion.

If we compare buoyancy to surface tension forces (the Bond number B), we see that buoyancy dominates slightly in our experiments (B > 1) but that surface tension clearly dominates in magma (B ≪ 1). This means that bubbles rising freely in the liquid will deform more easily in our setup, whereas we expect that freely rising bubbles in magma will be spherical unless they are very large. The capillary number Ca, which is the ratio of viscous forces to surface tension forces (note that Ca = We/Re), is similar in magnitude to the Bond number. This can be expected based on the fact that inertia forces are small in both systems and buoyancy forces and viscous forces therefore balance each other. In our experiments Ca ≈ 1, indicating that both viscous and surface tension forces are important. Ca increases with bubble size, and this is reflected in our observation that larger bubbles deform more than smaller ones. Surface tension is more important in Stromboli magma, where Ca ≪ 1, and we therefore expect bubbles to deform less easily in magma than in our experimental setup.

From this comparison, we infer that most of the bubble deformation observed in our tephra samples probably results from bubble expansion caused by rapid decompression on eruption, hindered by crystals present in the magma, rather than during bubble rise prior to eruption. The bubble marked by an x in Fig. 6c, for example, could have been spherical and positioned centrally between the three crystals, and could then have expanded outwards against the crystals on eruption. In this case, the observed deformation would indicate restricted lateral crystal movement, consistent with the high crystallinity and rapid magma quenching. In some cases, however, the observed bubble deformation appears too extensive to result entirely from crystal-hindered expansion. The bubble marked by an x in Fig. 6d, for example, could presumably have expanded more easily into the now glassy area towards the bottom of the figure instead of deforming around the plagioclase crystal. Bubble textures such as these suggest that, although most of the deformation probably happened on eruption, some could have happened in the conduit by processes similar to those in our experiments, although over longer time scales. We expect that, even though the deformability of bubbles

is small in magma, some bubbles are rising through the magma and deforming, as discussed in the next section.

5. The role of gas in Strombolian eruptions

5.1. Gas migration through magma

Bubbles seen in tephra from Stromboli either nucleated in situ or migrated to their current location from deeper in the magmatic system. As the gas flux far exceeds the amount of magma ejected (Harris and Ripepe, 2007), a large volume of gas has to pass through the upper part of the magma column with only minimal entrainment of the magma. Several conceptual models exist for how this gas moves through. For example, Burton et al. (2007) suggest that permeable pathways may begin to develop at several km depth and enable gas to be transported directly to the surface. In this model, small bubbles result from late-stage nucleation, and deformed bubbles result from coalescence that ultimately produces a 3D permeable network all the way through the crystal-rich magma. Lautze and Houghton (2006) assume that small spherical bubbles result from late-stage nucleation, and larger deformed bubbles result from coalescence of smaller bubbles. They notice that these larger bubbles can be aligned along boundaries between parts of their samples with different textures and conclude that these bubbles may be able to migrate through the melt phase. They also hypothesize that mixing of the different magmas represented by the different textures in their samples is aided by migration of small bubbles from one magma to the other. In all models, some gas is expelled as large gas slugs during Strombolian eruptions. These bubbles, which are several orders of magnitude larger than the crystals, will have to push the liquid-crystal mixture aside to rise through. The effect of crystals in this case will be to increase the effective viscosity of the mixture relative to the viscosity of the liquid phase alone. Such large bubbles cannot be studied from eruptive products as they are larger than the tephra or pumice clasts and are therefore not preserved in the samples. Here, we study the effect of crystals on bubbles that are similar in size to the crystals, such as those found in thin sections from Stromboli (e.g. Fig. 5).

If bubbles are small and if the crystal concentration is high, which is the case for the bubble populations preserved in Stromboli tephra, bubbles rise primarily by displacing the liquid rather than the liquid-crystal mixture. In this case, the viscosity to consider is the actual liquid viscosity rather than the effective viscosity of the mixture. Because the crystals occupy space that is unavailable for the bubbles to move into, bubbles must deform or not move at all. At Stromboli, passive degassing is widespread, indicating that gas is percolating through the crystal-rich system. Unless permeable networks are formed all the way down through the crystal-rich magma, some bubbles will have to migrate through the system, and, if they are

Table 2
Comparison of dimensionless parameters for our analogue system and Stromboli magma. d, w, ρ, η, σ: see Table 1; g: acceleration of gravity; r: bubble radius (d/2); u: bubble velocity. See text for discussion.

	Definition	Analogue (light syrup)	Stromboli
ψ	d/w	0.8–1.8	0.3–3
Re	$\rho r u/\eta$	0.0053–0.036	10^{-11}–10^{-9}
We	$\rho r u^2/\sigma$	0.002–0.038	10^{-15}–10^{-12}
B	$\rho g r^2/\sigma$	1.5–7.0	10^{-5}–10^{-2}
Ca	$\eta u/\sigma$	0.33–1.06	10^{-5}–10^{-3}

larger than the size of the pores between the crystals, these will have to deform to move through. Persistent percolating pathways are most likely to occur in shallow crystal-rich magma, which approaches conditions of porous media flow. The discrete nature of the active degassing (puffing) activity at Stromboli implies that permeable pathways may not stay open continuously, even at shallow depth. We envisage a model in which a transient permeable network may exist in the very upper part of the conduit (the opening and closing of which may give rise to puffing activity), but gas percolating through the deeper regions must be rising as bubbles. In addition, we expect that small bubbles will accumulate in near-surface, crystal-rich magma. This may explain the anomalously high small bubble population in Stromboli scoria compared to its low mass eruption rate (Mastin, 1997 and Figure 16 in Houghton and Gonnermann, 2008).

5.2. Bubble populations as a proxy for gas flux

We have shown that bubble populations are influenced by particles in suspensions with high concentrations of solids. Splitting of large bubbles around particles causes enrichment of small bubbles at the expense of larger ones in our experiments, although this effect might not be as important in magmatic systems, where bubbles deform less easily. Trapping of small bubbles by particles will also increase the number of small bubbles in the suspension. Chemical engineering experiments show that gas holdup increases with increasing gas flux, even in the absence of particles (e.g. Aslan et al., 2006). An increase in gas holdup can be manifested as an increase in bubble size or an increase in the number of bubbles present at any one level in the system. We use literature data to demonstrate the linkage between gas flux and explosivity at Stromboli volcano and investigate how bubble size distribution data might contribute to understanding the role of gas flux in light of our analogue experiments.

As discussed above, at Stromboli, three types of gas-driven activity occur simultaneously: Strombolian eruptions, active degassing (puffing) and passive degassing. As gas flux far exceeds magma flux, we can conclude that gas flux is the main factor driving normal activity. Ripepe et al. (2002) distinguish two phases of explosive degassing with different intensities, based on thermal and infrasonic data. During higher-intensity phases, Strombolian explosions are frequent and puffing is rapid but individual puffs are short. During lower-intensity phases, Strombolian explosion frequencies are lower and puffs are longer but less frequent. Different delay times between infrasonic and thermal signals during these two phases indicate higher gas jet velocities and/or elevated magma free surface levels during the higher-intensity phases.

Volcanic clasts are formed during gas-driven, normal Strombolian activity when fragments of magma are expelled by gas bubbles as they burst at the magma free surface. Ripepe et al. (2002, 2008) report correlations between the frequency of explosions, the gas jet velocity, and the magma free surface level. Ripepe et al. (2008) interpret these correlations to reflect changes in gas flux into the shallow system. Addition of gas into the shallow system would raise the level of the magma free surface in the conduit. Changes in eruption frequency (and resulting mass ejection rates) would reflect this increase in gas flux (e.g. Chadwick et al., 2008). This model could be tested by examining bubble populations in tephra erupted during periods of different eruptive intensity. Tephra erupted during periods of high gas supply rate should record an increase in gas holdup in the system, similar to the change in gas holdup with gas flux observed in chemical engineering studies (e.g. Aslan et al., 2006).

The only published study that provides detailed data on bubble populations in tephra as a function of eruption intensity is that of Colò et al. (2010), who show that bubble number densities vary inversely with infrasonic amplitude (a measure of eruptive intensity). These data are interesting as this trend is the opposite of that predicted by vesiculation models, where an increase in eruption intensity would be expected to cause an increase in the effective pressure driving vesiculation, which in turn should increase rates of bubble nucleation over bubble growth (e.g. Mastin et al., 2004). Colò et al. (2010) explain this relationship by suggesting that higher gas contents in the rising magma would allow more efficient coalescence and hence larger and more frequent explosions. They do not address the source of changing gas contents within the column, nor do they report the bulk vesicularity of the samples, which would be the most direct measure of gas holdup. Since gas holdup should increase with increasing gas flux, finding a proxy for gas holdup in volcanic samples would allow us to extract information on the gas flux at the time the samples were erupted, unless other factors, unrelated to gas flux, also affect holdup.

Factors that might affect gas holdup in the absence of a change in gas flux are crystal concentration and crystal size. Our experiments suggest that an increase in crystal concentration could facilitate trapping of small bubbles within the suspension and thus increase gas holdup. Likewise, increasing crystal size might enable larger bubbles to stagnate, and increase gas holdup. However, crystal size distributions for Stromboli tephra (Armienti et al., 2007; Cigolini et al., 2008) show no obvious correlation between vesicularity and crystal concentration or number-referenced dominant crystal size (both calculated from crystal size distributions according to Cashman and McConnell, 2005). Thus it appears that changes in the bubble population with eruptive intensity at Stromboli must be explained either by changes in bubble nucleation and growth rates (Ripepe et al., 2002) or by changes in gas flux from depth (Ripepe et al., 2008; implied by Colò et al., 2010). Our data support the latter interpretation, and suggest that the high crystallinity of the shallow Stromboli magma plays a critical role in modulating gas flux through the system. Gas flux is an important parameter driving volcanic eruptions. Establishing links between gas flux and bubble populations could provide a way of tracking changes in gas flux in crystal-rich systems through their deposits and improve our understanding of the mechanisms of gas migration that give rise to passive degassing.

6. Conclusions

We have performed analogue experiments to determine the effect of solid particles on bubble shapes and sizes as they rise through a suspension with high (~50%) solids concentration, and have used our experimental results to interpret bubble populations in crystal-rich tephra from Stromboli volcano, Italy. We find that particles can cause bubbles to deform and split, providing alternative interpretations to coalescence and late-stage nucleation (e.g. Lautze and Houghton, 2006; Polacci et al., 2006a; Shimano and Nakada, 2006) for large deformed bubbles and small spherical bubbles observed in crystal-rich tephras. Relative enrichment of small bubbles due to trapping within particle-rich suspensions implies that bubble number densities may not be direct representations of bubble nucleation rates in crystalline magmas. Instead, bubble splitting around particles could increase the relative abundance of small bubbles in the system, as could accumulation of small bubbles within the magma because of trapping. A comparison of the relative importance of the forces acting on the bubbles in our experiments and in Stromboli magma indicates that most of the bubble deformation observed in tephra probably results from bubble expansion on eruption, although bubble textures (e.g. Fig. 6d) suggest that some deformation occurred in the magma prior to eruption.

Other low viscosity, crystal-rich magmas to which our experimental results could be applied include Mount Etna, Italy (where Polacci et al., 2006b, report vesicle-free phenocryst crystallinities of 25–40%) and Villarrica, Chile (where Gurioli et al., 2008, report vesicle-free phenocryst crystallinities up to 56.4%). In addition to volcanic systems, our experiments may provide useful insights into

mechanisms of gas transport in other particle-rich systems, such as crystallizing plutons and marine sediments.

Acknowledgements

Appendix A. Supplementary data

Supplementary data associated with this article can be found, in the online version, at doi:10.1016/j.epsl.2010.06.014.

References

Abramoff, M.D., Magelhaes, P.J., Ram, S.J., 2004. Image processing with Image. J. Biophoton. Int. 11 (7), 36–42.

Armienti, P., Francalanci, L., Landi, P., 2007. Textural effects of steady state behaviour of the Stromboli feeding system. J. Volcanol. Geoth. Res. 160, 86–98.

Aslan, M.M., Crofcheck, C., Tao, D., Mengüç, M.P., 2006. Evaluation of micro-bubble size and gas hold-up in two-phase gas-liquid columns via scattered light measurements. J. Quant. Spectrosc. Radiative Transf. 101, 527–539.

Bagdassarov, N., Dorfman, A., Dingwell, D.B., 2000. Effect of alkalis, phosphorus, and water on the surface tension of haplogranite melt. Am. Mineral. 85, 33–40.

Bertagnini, A., Métrich, N., Landi, P., Rosi, M., 2003. Stromboli volcano (Aeolian Archipelago, Italy): An open window on the deep-feeding system of a steady state basaltic volcano. J. Geophys. Res. 108 (B7), 2336. doi:10.1029/2002JB002146.

Burton, M.R., Mader, H.M., Polacci, M., 2007. The role of gas percolation in quiescent degassing of persistently active basaltic volcanoes. Earth Planet. Sci. Lett. 264, 46–60.

Cashman, K.V., McConnell, S.M., 2005. Multiple levels of magma storage during the 1980 summer eruptions of Mount St. Helens, WA. Bull. Volcanol. 68, 57–75.

Cashman, K.V., Mangan, M.T., Newman, S., 1994. Surface degassing and modifications to vesicle size distributions in Kilauea basalt. J. Volcanol. Geotherm. Res. 61, 45–68.

Chadwick Jr., W.W., Cashman, K.V., Embley, R.W., Matsumoto, H., Dziak, R.P., de Ronde, C.E.J., Lau, T.K., Deardorff, N.D., Merle, S.G., 2008. Direct video and hydrophone observations of submarine explosive eruptions at NW Rota-1 volcano, Mariana arc. J. Geophys. Res. 113. doi:10.1029/2007JB005215 B08S10.

Cigolini, C., Laiolo, M., Bertolino, S., 2008. Probing Stromboli volcano from the mantle to paroxysmal eruptions. In: Annen, C., Zellmer, G.F. (Eds.), Dynamics of Crustal Magma Transfer, Storage and Differentiation: Geological Society, London, Special Publications, 304, pp. 33–70.

Colò, L., Ripepe, M., Baker, D.R., Polacci, M., 2010. Magma vesiculation and infrasonic activity at Stromboli open conduit volcano. Earth Planet. Sci. Lett. 292, 274–280.

Gurioli, L., Harris, A.J.L., Houghton, B.F., Polacci, M., Ripepe, M., 2008. Textural and geophysical characterization of explosive basaltic activity at Villarrica volcano. J. Geophys. Res. 113, B08206. doi:10.1029/2007JB005328.

Harris, A., Ripepe, M., 2007. Temperature and dynamics of degassing at Stromboli. J. Geophys. Res. 112, B03205. doi:10.1029/2006JB004393.

Houghton, B.F., Gonnermann, H.M., 2008. Basaltic explosive volcanism: constraints from deposits and models. Chem. Erde 68, 117–140.

Khitarov, N.I., Lebedev, Ye.B., Dorfman, A.M., Bagdasarov, N.Sh., 1979. Effects of temperature, pressure, and volatiles on the surface tension of molten basalt. Geochem. Int. 16 (5), 78–86.

Landi, P., Métrich, N., Bertagnini, A., Rosi, M., 2004. Dynamics of magma mixing and degassing recorded in plagioclase at Stromboli (Aeolian Archipelago, Italy). Contrib. Mineral. Petrol. 147, 213–227.

Landi, P., Métrich, N., Bertagnini, A., Rosi, M., 2008. Recycling and "re-hydration" of degassed magma inducing transient dissolution/crystallization events at Stromboli (Italy). J. Volcanol. Geotherm. Res. doi:10.1016/j.jvolgeores.2008.02.013.

Lautze, N.C., Houghton, B.F., 2006. Linking variable explosion style and magma textures during 2002 at Stromboli volcano, Italy. Bull. Volcanol. doi:10.1007/s00445-006-0086-1.

Mangan, M., Sisson, T., 2005. Evolution of melt-vapor surface tension in silicic volcanic systems: experiments with hydrous melts. J. Geophys. Res. 110, B01202. doi:10.1029/2004JB003215.

Mastin, L.G., 1997. Evidence for water influx from a caldera lake during the explosive hydromagmatic eruption of 1790, Kilauea volcano, Hawaii. J. Geophys. Res. 102 (B9), 20093–20109.

Mastin, L.G., Christiansen, R.L., Thornber, C., Lowenstern, J., Beeson, M., 2004. What makes hydromagmatic eruptions violent? Some insights from the Keanakako'i ash, Kīlauea Volcano, Hawai'i. J. Volcanol. Geotherm. Res. 137, 15–31.

Mena, P.C., Ruzicka, M.C., Rocha, F.A., Teixeira, J.A., Drahos, J., 2005. Effect of solids on homogeneous–heterogeneous flow regime transition in bubble columns. Chem. Eng. Sci. 60, 6013–6026.

Métrich, N., Bertagnini, A., Landi, P., Rosi, M., 2001. Crystallization driven by decompression and water loss at Stromboli volcano (Aeolian Islands, Italy). J. Petrol. 42 (8), 1471–1490.

Polacci, M., Baker, D.R., Mancini, L., Tromba, G., Zanini, F., 2006a. Three-dimensional investigation of volcanic textures by X-ray microtomography and implications for conduit processes. Geophys. Res. Lett. 33, L13312. doi:10.1029/2006GL026241.

Polacci, M., Corsaro, R.A., Andronico, D., 2006b. Coupled textural and compositional characterization of basaltic scoria: insights into the transition from Strombolian to fire fountain activity at Mount Etna, Italy. Geology 34 (3), 201–204.

Ripepe, M., Harris, A.J.L., Carniel, R., 2002. Thermal, seismic and infrasonic evidences of variable degassing rates at Stromboli volcano. J. Volcanol. Geotherm. Res. 118, 285–297.

Ripepe, M., Marchetti, E., Ulivieri, G., 2007. Infrasonic monitoring at Stromboli volcano during the 2003 effusive eruption: insights on the explosive and degassing process of an open conduit system. J. Geophys. Res. 112, B09207. doi:10.1029/2006JB004613.

Ripepe, M., Delle Donne, D., Harris, A., Marchetti, E., Ulivieri, G., 2008. Dynamics of Strombolian activity. In: Calvari, S., Inguaggiato, S., Puglisi, G., Ripepe, M., Rosi, M. (Eds.), The Stromboli volcano: An integrated study of the 2002–2003 eruption: AGU Geophysical Monograph Series, Washington D.C., 182, pp. 39–48.

Shaw, H.R., 1972. Viscosities of magmatic silicate liquids: an empirical method of prediction. Am. J. Sci. 272, 870–893.

Shimano, T., Nakada, S., 2006. Vesiculation path of ascending magma in the 1983 and the 2000 eruptions of Miyakejima volcano, Japan. Bull. Volcanol. 68, 549–566.

Spera, F.J. (2000). Physical properties of magma. In: Encyclopedia of Volcanoes, Ed.-in-Chief: H. Sigurdsson, Academic Press, 171–190.

Vergniolle, S. and Mangan, M. (2000). Hawaiian and Strombolian eruptions. In: Encyclopedia of Volcanoes, Ed.-in-Chief: H. Sigurdsson, Academic Press, 447–461.

Web reference: http://www.ct.ingv.it/stromboli2007/main.htm (description of activity per day (in Italian), accessed 5 January 2010).